CO2-switchable thermoresponsiveness of poly(N,N-(diethylamino)ethyl acrylamide)-based homo- and copolymers in water

Fang Yin, Barbara Lonetti, Jean-Daniel Marty, Nancy Lauth-de Viguerie

CO_2-switchable thermoresponsiveness of poly(*N*,*N*-(diethylamino)ethyl acrylamide)-based homo- and copolymers in water

Fang Yin, Barbara Lonetti, Jean-Daniel Marty* and Nancy Lauth-de Viguerie*

Laboratoire des IMRCP, CNRS UMR 5623, Université de Toulouse, UPS, 118 route de Narbonne, F-31062 Toulouse, France.

* Corresponding authors:

E-mail addresses: nancy.de-viguerie@univ-tlse3.fr, jean-daniel.marty@ univ-tlse3.fr;

GRAPHICAL ABSTRACT

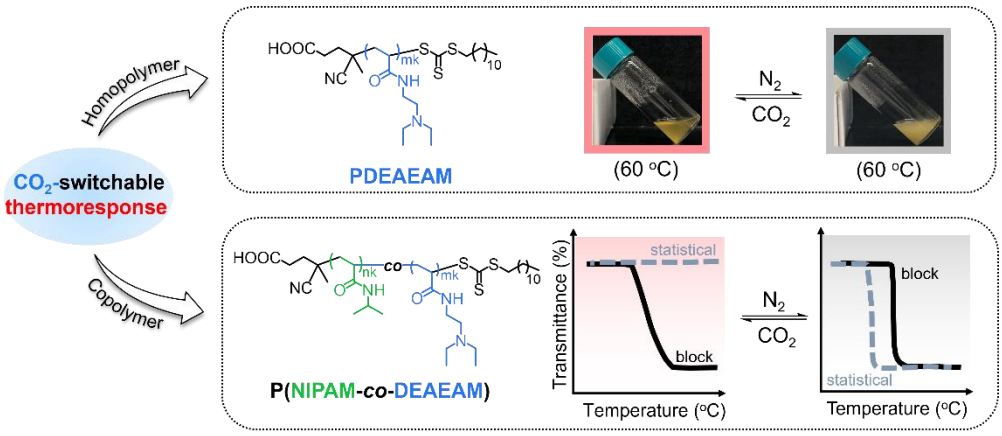

The insertion of CO_2 switchable *N*,*N*-(diethylamino)ethyl acrylamide monomer enable to tune easily and reversibly the properties of PNIPAM-based polymers.

ABSTRACT

The properties of thermo-sensitive polymers can be easily and reversibly switched using addition/removal of carbon dioxide (CO_2) as an innovative and ecological trigger. *N*,*N*-(diethylamino)ethyl acrylamide (DEAEAM) was (co)polymerized with *N*-isopropylacrylamide (NIPAM) by Reversible Addition-Fragmentation chain Transfer (RAFT) polymerization to obtain copolymers with various compositions and architectures. The properties (solubility, aggregation behavior…) of these polymers in aqueous solution in the presence of CO_2 was studied via scattering, microscopy and turbidimetry measurements. The copolymerization of *N*,*N*-(diethylamino)ethyl acrylamide (DEAEAM) monomer with NIPAM enables to produce either a statistical copolymer or a series of diblock copolymers and to tune the cloud point temperature of obtained copolymers either by changing the composition or the architecture (statistical, block) or by CO_2 addition/removal. Whereas, for a given composition, statistical copolymer does not display thermoresponsive behavior, block copolymers present a thermoresponsiveness which depends on the protonation degree of tertiary amine functions. Additionally, CO2 can be used to reversibly modulate the properties of these materials in aqueous media.

KEYWORDS: CO_2-responsive block copolymers, pH and thermo-responsive block copolymers, RAFT, PNIPAM, tertiary amine moieties

1. Introduction

Carbon dioxide (CO_2) has emerged as an innovative and green trigger for switching the properties (such as solubility, dimension, chain conformation, morphology, shape...) of responsive polymer materials in aqueous media. [1-5] As a key metabolite in living organisms, CO_2 displays excellent biocompatibility and membrane permeability; as an industrial production waste, it is abundant, inexpensive, available and nontoxic. Moreover, in aqueous solution, CO_2 combines with water to form carbonic acid, which lowers the solution pH. The added CO_2 can be easily removed by bubbling inert gases, e.g. nitrogen or argon, or by heating up the solution [6] causing the polymer return back to its original state. Therefore, CO_2-reponsiveness is a special example of a pH-responsive trigger. Generally, in classical pH-responsive systems, an acid or a base solution is added to trigger the property change, which leads to the accumulation of salt in system. However, such salt build-up can be avoided by using CO_2. [3,5,7] Thus, developing CO_2-responsive polymer materials holds great promise for designing switchable vectors in drug delivery, [8,9] for limiting CO_2 emission from industrial process [10-11] and for controllably separating oil/water mixture. [12,13]

Commonly reported CO_2-responsive polymer materials comprise amidine, [14,15] guanidine, [16] imidazole [17] and amine groups. [18-20] These functions in aqueous media can react with CO_2 to generate charged species. However, the switching between neutral and charged forms upon CO_2 addition/removal is not always fully reversible. [21] Thus, moderately basic tertiary amine-based polymers exhibit reversible behavior, whereas those with a strong or weak basicity cannot be easily recovered to neutral forms or are less sensitive to CO_2 stimulation. Hence polymers with tertiary amines functional groups are readily switched to bicarbonate salt upon CO_2 exposure and return to neutral form after exposure to inert gases.

Some amine-based CO_2-responsive homopolymers, mostly in their uncharged forms, display thermoresponsive behaviors. Among them, poly(*N*,*N*-(dimethylamino)ethyl methacrylate) (PDMAEMA) (p*K*a ~ 7.5) and poly(*N*,*N*-(diethylamino)ethyl methacrylate) (PDEAEMA) (p*K*a ~ 7.4) are the most studied CO_2-responsive polymers since their corresponding monomers are commercially available. [22, 23]

PDMAEMA and PDEAEMA exhibit a lower critical solution temperature (LCST) within a specific pH window. The number of carbon atoms in alkyl substituent (methyl or ethyl) has a pronounced effect on the value of transition temperature: PDMAEMA is well soluble in water at room temperature whatever the pH value and presents a LCST behavior only at high pH values (above p*K*a). In contrast, PDEAEMA is soluble and thermoresponsive in its protonated form and is no longer soluble at high pH whatever the temperature. [24] Copolymers based on these two CO_2-responsive polymers have thus been extensively studied for their ability to form different colloidal structures (nanospheres, gels, micelles, polymersomes…) and to induce reversible morphological transition upon CO_2 exposure from a simple volume change to a sol-to-gel or micelle-to-vesicle transition. [20,25-27]

Poly(*N*-isopropylacrylamide) (PNIPAM) presents, like poly(*N*-vinylcaprolactam) [28,29] or poly(oligo(ethylene glycol) methyl ether (meth)acrylate)s, [30] a thermoresponsive character which is materialized by the presence of a LCST in its phase diagram. This results from a coil-to-globule transition due to the dehydration of polymer chains at temperature around 32 °C. [31-33] The incorporation of hydrophilic or hydrophobic comonomers into PNIPAM allows fine-tuning of the cloud point temperature (T_c). [34,35] Therefore, the objective here is to insert into PNIPAM structure CO_2-responsive moieties, whose hydrophilicity can be modulated by addition/removal of CO_2, which will make it possible to play on the thermosensitive properties of the considered polymers. Therefore, previous studies described the synthesis of PNIPAM-based CO_2-responsive copolymers with diblock (PDEAEMA$_{60}$-*b*-PNIPAM$_{40}$) [36], triblock (PNIPAM-*b*-PCL-*b*-PDMAEMA with PCL corresponding to poly(ε-caprolactone)) [37] or more complex structures (PCL-*b*-P(NIPAM-*co*-DMAEMA) with a pyrene termination group).[38]

With the objective to insert such CO_2-sensitive groups in PNIPAM, the use of monomers based on acrylamide is of special interest compared to the poly(methacrylate) monomers: a higher hydrolytic stability during heating/cooling cycles at different pH values and a radical reactivity close to the

one of PNIPAM. **Scheme 1** illustrates CO_2-responsive poly((meth)acrylamide) polymers reported in the literature.

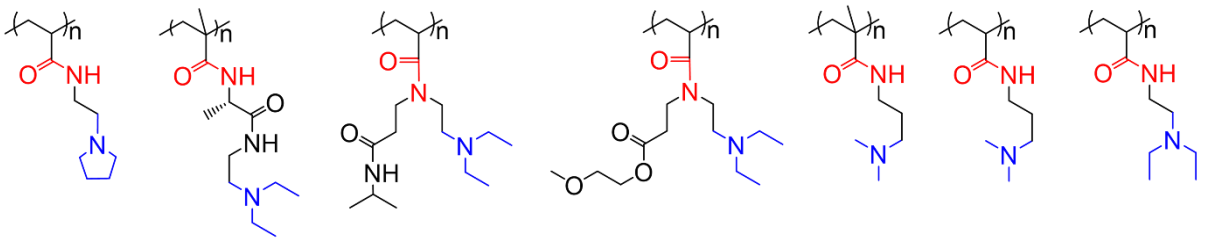

Scheme 1. Chemical structures of *N*-substituted poly((meth)acrylamide)s with CO_2-responsiveness. (PEPyAM: poly(*N*-ethylpyrrolidine acrylamide), [39] PMAEE: poly(*N*-methacryloyl-L-alanine 2-(diethylamino) ethylamide), [40] P(DEAE-NIPAM-AM): poly(*N*-(2-(diethylamino) ethyl)-*N*-(3-(isopropylamino)-3-oxopropyl) acrylamide), [41] P(MEO-DEAE-AM): poly(2-methoxyethyl 3-(*N*-(2-diethylamino ethyl) acrylamido) propanoate), [42] PDMAPMAM: poly((*N*,*N*-dimethylamino)propyl methyl acrylamide), [43] PDMAPAM: poly((*N*,*N*-dimethylamino)propyl acrylamide), [44] PDEAEAM: poly((*N*,*N*-diethylamino)ethyl acrylamide). [45]

Among them, PDEAEAM homopolymer which is thermo- and pH-/CO_2-responsivis is of special interest. PDEAEAM is thermoresponsive in its unprotonated form and lose this property in its protonated form upon CO_2 bubbling. Bubbling inert gases enable to recover partially its thermoresponsiveness depending on the final protonation degree of the tertiary amine: hence T_c value decrease from 50.2 to 33.1 ^oC when the pH increases from 8.5 to 11.[45]. However, literatures involving multi-stimuli responsiveness of PDEAEAM-based copolymers are relatively scarce. Guan and co-workers designed a multi-stimuli responsive star polymer of tetraphenylethene-*graf*-tetra-poly(*N*,*N*-(diethylamino) ethyl) acrylamide), which displayed a good performance in long-term cell tracing. [46] Kim et al. employed P(DEAEAM-*r*-NIPAM) as responsive surfactant to

modulate shape transition of poly(styrene)-*b*-poly(4-vinylpyridine) particles between football and lens over a subtle change of temperature and pH. [48]

In this work, the objective is to evaluate how copolymer composition and architecture affect the thermoresponsive properties and the aggregation behavior of PDEAEAM-based copolymers (**Scheme 2**). A statistical copolymer P(NIPAM-*stat*-DEAEAM) and a series of block copolymers PNIPAM-*b*-PDEAEAM with variable compositions were synthesized by Reversible Addition-Fragmentation chain Transfer (RAFT) polymerization, their solubilities in water as well as the self-assembly behavior driven by temperature upon CO_2 addition/removal were then explored.

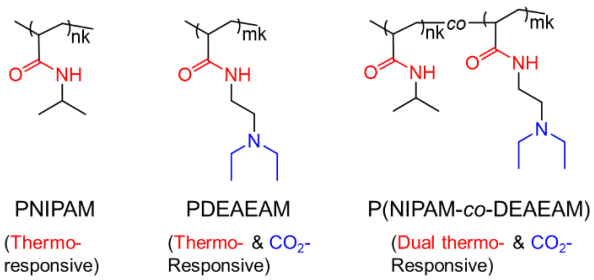

Scheme 2. Structure of PNIPAM and PDEAEAM homopolymers, as well as P(NIPAM-*co*-DEAEAM) copolymer.

2. Materials and methods

2.1. Reagents

N-isopropylacrylamide monomer (NIPAM, Sigma-Aldrich), 4-cyano-4-((dodecylsulfanylthiocarbonyl) sulfanyl) pentanoic acid (CDTPA, 97%, Sigma-Aldrich) were used as received. 2,2'-Azobis(isobutyronitrile) (AIBN) was recrystallized twice from methanol. *N*,*N*-(diethylamino)ethyl acrylamide (DEAEAM) was synthesized as described elsewhere [43]. 1,4-Dioxane was purified by passing through alumina column prior to use. All other reagents were used as received unless otherwise specified. Ultrapure water with a resistivity of 18.2 MΩ·cm was obtained using a Purelab Flex 1 apparatus.

2.2. Characterization

2.2.1. Nuclear Magnetic Resonance Spectroscopy (NMR). ^{1}H NMR spectra were recorded on Bruker Advance spectrometers (300 or 500 MHz) with D_2O as the solvent and 1,3,5-trioxane was used as an internal standard. The theoretical molecular weights ($M_{n,theo}$) of synthesized (co)polymers were calculated by (**eq. 1**):

$$M_{n,theo} = \frac{[M]_0 \times M_M \times Conv.}{[CTA]_0} + M_{CTA} \qquad \textbf{(eq. 1)}$$

Where $[M]_0$ and $[CTA]_0$ are initial concentrations of monomer and chain transfer chain agent, respectively. M_M and M_{CTA} are molecular weights of monomer and chain transfer agent, respectively. Conv. is the monomer conversion determined by ^{1}H NMR spectra.

2.2.2. Size exclusion chromatography (SEC). Molecular weights and molecular weight distributions of all the polymers were determined on a SEC apparatus composed of a MALVERN multi-angle light scattering detector (MALS), a Waters 2140 refractive index (RI) detector and UV detector via using a Styragel HR4E column. Samples were prepared with a concentration of 10 mg·mL^{-1} and filtered through 0.45 μm PTFE filters. DMF (containing 10 mM LiBr) and THF (containing 2 vol.% TEA) were both used as eluents with a flow rate of 1 mL·min^{-1} at 35 °C. The molecular weight was studied from the knowledge of dn/dc value measured in DMF (containing 10 mM LiBr): $[dn/dc]_{PN}$ = 0.08598 mL·g^{-1} (PN stands for PNIPAM), $[dn/dc]_{PD}$ = 0.09715 mL·g^{-1} (PD stands for PDEAEAM); in THF with 2 vol.% TEA: $[dn/dc]_{PN}$ = 0.1131 mL·g^{-1}, $[dn/dc]_{PD}$ = 0.1057 mL·g^{-1}), which was measured by using a DNDC- 2010 differential refractometer (PSS) at 620 nm. For the block copolymers, the refractive index increments (dn/dc) value were calculated using (**eq. 2**):

$$dn/dc = w_A \times (dn/dc)_A + w_B \times (dn/dc)_B \qquad \textbf{(eq. 2)}$$

2.2.3. Differential Scanning Calorimetry (DSC). Glass transition temperatures (T_g) of bulk (co)polymers were measured on heating (heating rate: 10 $^oC \cdot min^{-1}$) on a Mettler Toledo DSC 1 STARe System Thermal Analysis calorimeter with a Gas Controller GC200.

2.2.4. Dynamic light scattering (DLS). Dynamic light scattering (DLS) measurements were carried out on Zetasizer Nano-ZS (Malvern Instruments, Ltd, UK), with a 4 mW He-Ne laser (λ = 633 nm, light scattering measured at 173°). The correlation function was analyzed via the cumulant method to get the Z-average diameter of the colloids and by the general purpose method (NNLS) to obtain the distribution of diffusion coefficients of the solutes. The apparent equivalent hydrodynamic diameter was then determined using the Stokes–Einstein equation. Standard deviations were evaluated from diameter distribution. Zeta potential values of aggregates were obtained by doppler anemometry technique, and the test process requires an electric field to be applied to the entire sample solution. This process performed on Zetasizer Nano-ZS (Malvern Instruments, Ltd, UK) using folded capillary cells (DTS 1070) at 25 °C.

2.2.5. Turbidimetry measurements. The transmittance of (co)polymer solution was recorded on a variable UV-visible spectrophotometer at 500 nm under continuous stirring with a heating rate of 1 $^oC \cdot min^{-1}$. The cloud point temperature (T_c) was obtained either by the inflection point ($T_{c,ip}$) on transmission curves or by the temperature ($T_{c,onset}$) at which the transmittance of solution begins to decrease.

2.2.6. Transmission electron microscopy (TEM).

TEM observations were performed on a MET hitachi HT7700 instrument at an accelerating voltage of 80 kV**.** Samples were prepared in a dry box with setting temperature of 25 or 60 ^oC. Copolymer solution, copper grids and pipette tips were preheated in the dry box for 20 min. A 6 µL drop of the copolymer solution was deposited onto the copper grid until the solvent was evaporated, then these samples were

stained with 2 wt.% uranyl acetate solution preheated at the sample temperature. After 2 min, the excess solution was removed by filter paper and samples were dried again. **Note**: to prepare samples in the presence of CO_2 or N_2, copolymer solution was bubbled with CO_2 or N_2 at room temperature with a flow rate of 10 $min \cdot L^{-1}$ for 10 min or 30 min, respectively, and sealed with rubber caps. Then samples at different temperatures were prepared with the similar procedures but a CO_2 or N_2 flow was employed during the drying process.

2.2.7. Small Angle X-rays scattering (SAXS) on 1 wt.% PN_{5k}-*b*-PD_{5k} solution was performed with a XEUSS 2.0 SAXS/WAXS laboratory beamline equipped with a Cu source (E = 8 keV). The 2D SAXS patterns were collected using a pixel detector PILATUS3 1 M from Detrics. The sample to detector distance was 1216.5 mm (beam size 0.8 × 0.8 mm), covering a *q*-range from 0.007 to 0.5 $Å^{-1}$. q is the scattering wave vector defined as $q=(4\pi/\lambda)\sin\vartheta/2$, λ is the wavelength ($\lambda \sim 1.54$ Å) and ϑ is scattering angle. The solutions were loaded in borosilicate capillaries of 1.5 mm diameter in thermostatic sample holders. The SAXS curves were measured at 25 and 60 °C.

The model used to describe the curves at 25 °C as star-like assemblies is the one developed for star-polymers formed of gaussian polymer arms: [49]

$$I(q) = \frac{2}{f\nu^2}\left[\nu - 1 + e^{-\nu} + \frac{f-1}{2}(1 - e^{-\nu})^2\right] \qquad \textbf{(eq. 3)}$$

$$\nu = \frac{\langle R_g^2 \rangle q^2 f}{(3f-2)} \qquad \textbf{(eq. 4)}$$

with $\langle R_g^2 \rangle$ is the square of the ensemble average gyration radius of the full assembly and f is the number of arms of the self-assembly.

The scattering curve of the sample at 60 °C upon CO_2 treatment was described using the model of (**eq. 5**) [50] formed by two terms, the first one describes the Porod scattering from clusters, while the second one is a Lorentzian function describing the scattering from polymer chains.

$$I(q) = \frac{A}{q^m} + \frac{B}{1+(\xi q)^n} \qquad \textbf{(eq. 5)}$$

A and B are two scale constants, m is the Porod exponent from the scattering of clusters, ξ and n are the correlation length and power law exponent of polymer chains, respectively. Best fits of the form factor $P(q)$ for the measured data were derived using the SASView program (http://www.sasview.org/).

2.2.8. pKa measurement. The p*K*a value of PD_{5k} homopolymer was determined by titration with a Mettler Toledo seven excellence pH meter. Prior to measurement, pH value of the studied solution ($1.76 \cdot 10^{-2}$wt%) was adjusted to 3 by addition of HCl solution (0.1 mol·L^{-1}) to ensure full protonation of tertiary amine group. Then the solution was titrated with NaOH solution (0.1 mol·L^{-1}). The value of p*K*a was determined by the inflection point on pH curve as a function of added volume of NaOH.

2.3. Synthesis

The desired PNIPAM and PDEAEAM homopolymers, and a series of PNIPAM-*b*-PDEAEAM block copolymers were synthesized by RAFT polymerization as previously described, [45-46] their corresponding synthetic procedures and characterizations were described in **Supporting Information** (scheme S1-S3 and Figures S1-S10).

Synthesis of poly((*N*-isopropylacrylamide)-*stat*-(*N,N*-(diethylamino)ethyl acrylamide)) (P(NIPAM$_{5k}$-*stat*-DEAEAM$_{5k}$)). NIPAM (1.00 g, 8.84 mmol), DEAEAM (1.00 g, 5.87 mmol), AIBN (0.017 g, 0.104 mmol), 4-cyano-4-((dodecylsulfanylthiocarbonyl) sulfanyl) pentanoic acid (CDTPA, 0.084 g, 0.208 mmol), 1,3,5-trioxane (0.053 g, 0.587 mmol, as an internal standard) and 1,4-dioxane (3.23 g) were added

into a Schlenk tube under argon flow, then the tube was immersed in a preheated oil bath at 70 ^{o}C. After a given time, the polymerization was stopped by rapidly cooling in liquid nitrogen, the desired statistical copolymer was collected by removing solvent, a subsequent precipitation in cold diethyl ether and drying under vacuum. Overall conversion: 98.5%, $M_{n,theo}$ = 9870 g·mol^{-1}, $M_{n,NMR}$ = 9460 g·mol^{-1}. In DMF (containing 10 mM LiBr): $M_{n,SEC}$ = 12060 g·mol^{-1}, Đ = 1.25. In THF (containing 2 vol.% TEA): $M_{n,SEC}$ = 7490 g·mol^{-1}, Đ = 1.34. ^{1}H NMR (500 MHz, D_2O) δ_H (ppm): 3.92 (s, 1H, -C<u>H</u>$(CH_3)_2$), 3.33 (s, 2H, -CONH-C<u>H</u>$_2$-), 2.64 (s, 6H, -N(C<u>H</u>$_2)_3$), 2.33 - 1.31 (m, -C<u>H</u>$_2$CH-CONH-, -CH$_2$C<u>H</u>-CONH-, -C(CN)-C<u>H</u>$_3$)-, -C<u>H</u>$_2$CH$_2$COOH, -CH$_2$C<u>H</u>$_2$COOH), 1.16 (s, 6H, -NHCH(C<u>H</u>$_3)_2$), 1.07 (s, 6H, -N(CH$_2$C<u>H</u>$_3)_2$), 0.89 (s, 3H, -$(CH_2)_{10}$-C<u>H</u>$_3$).

2.4. Gas aeration

A gas regulator was used to quantitatively control gas amount, CO_2/N_2 was introduced at room temperature by inserting a needle in (co)polymer solution with an appropriate flow rate at a given period of time.

3. Results and Discussion

3.1. Synthesis and characterization of (co)polymers.

PDEAEAM and PNIPAM reference homopolymers, as well as P(NIPAM-*co*-DEAEAM) copolymers with different architectures and compositions were synthesized by RAFT polymerization according to previously described synthetic pathways - using azobisisobutyronitrile (AIBN) as free-radical initiator and 4-cyano-4-((dodecylsulfanylthiocarbony) sulfanyl) pentanoic acid (CDTPA) as RAFT agent (**Scheme 3**). [45-46] These copolymers were designed with a targeted molecular weight of 10000 g·mol^{-1}.

All PDEAEAM$_{mk}$ homopolymer, PNIPAM$_{nk}$ homopolymer, PNIPAM$_{nk}$-*b*-PDEAEAM$_{mk}$ and P(NIPAM$_{nk}$-*stat*-DEAEAM$_{mk}$) copolymers discussed in this work are abbreviated as PD$_{mk}$, PN$_{nk}$, PN$_{nk}$-*b*-PD$_{mk}$ and P(N$_{nk}$-*stat*-D$_{mk}$) (mk and nk are molecular weights of PD and PN, respectively).

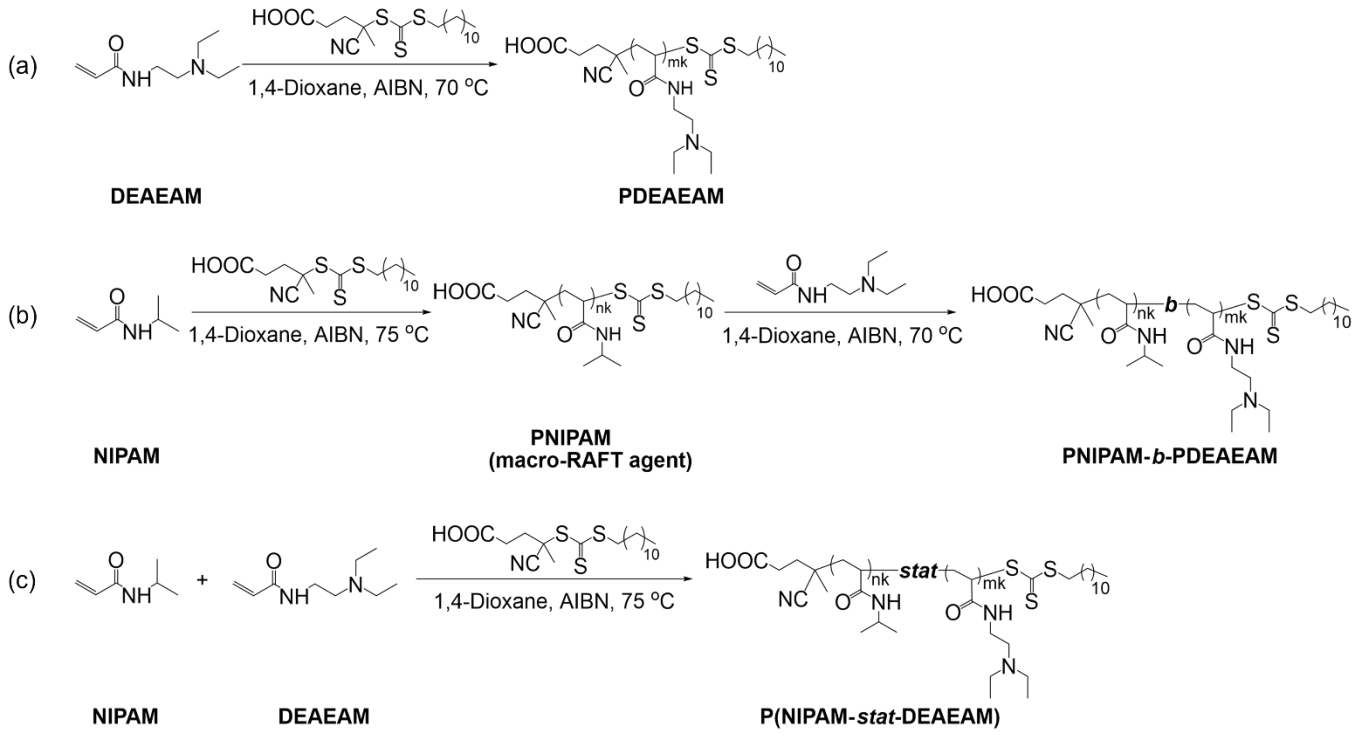

Scheme 3. Synthetic routes for preparation of (a) PDEAEAM homopolymer, (b) PNIPAM-*b*-PDEAEAM block copolymer and (c) P(NIPAM-*stat*-DEAEAM) statistical copolymer.

The successful copolymerization of DEAEAM and NIPAM was assessed by ^{1}H NMR experiments and size exclusion chromatography (SEC) analyses (**Figures S1 – S10)**. Hence, NMR spectra of all copolymers shows both characteristic peaks of the two polymerized monomers as illustrated in the case of P(N_{5k}-*stat*-D_{5k}) in **Figure 1a**. Moreover, in the case of block copolymers, diffusion-ordered spectroscopy (DOSY) experiments for PN_{5k}-*b*-PD_{5k} enables to determine a unique diffusion coefficient equal to 2.8 $m^2 \cdot s^{-1}$ (2.4×10^{-10} $m^2 \cdot s^{-1}$ in the case of PN_{5k}): the presence of remaining homopolymers is therefore neglectable.[46] Average number molecular weights (Mn) and dispersity (Đ) were evaluated by size exclusion chromatography (SEC) in DMF or THF. As shown in **Figure 1b**, a clear shift of elution peak of PN_{5k}-*b*-PD_{5k} and P(N_{5k}-*stat*-D_{5k}) towards high molecular weight is evidenced compared to macro-RAFT agent PN_{5k} in SEC chromatograms. However, in the cases of PD homopolymers and PN-b-PD block copolymers the interaction between the nitrogen-containing polymer and SEC columns hampers the precise determination of

molecular weights and induces the presence of a slight shoulder in DMF. [46] As a result, a clear shift of elution peak for block copolymers comprising a high content of PD compared to their macro-RAFT agent PN homopolymers is not always detected [51] whereas this phenomenon is considerably weakened in the case of P(N_{5k}-*stat*-D_{5k}). The main characteristics of synthesized polymers are summarized in **Table 1.**

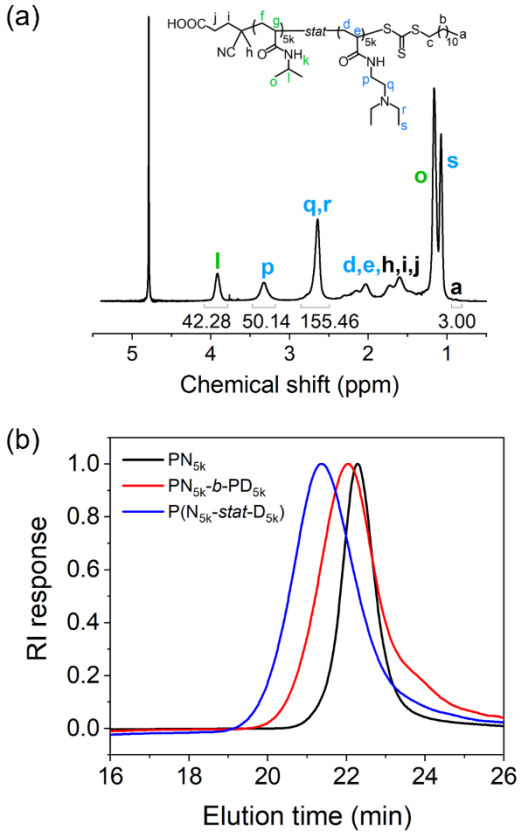

Figure 1. (a) ^{1}H NMR spectrum of P(N_{5k}-*stat*-D_{5k}) in D_2O and (b) SEC traces of PN_{5k}, PN_{5k}-*b*-PD_{5k} and P(N_{5k}-*stat*-D_{5k}) in DMF (containing 10 mM LiBr).

Table 1. (Co)polymers composition, glass transition temperature and average molecular weights

(Co)polymer	**DP_N:DP_D** [a]	T_g [a] (°C)	$M_{n,NMR}$ [a] (g·mol^{-1})	$M_{n,SEC}$ [c] (g·mol^{-1})	$M_{w,SEC}$ [c] (g·mol^{-1})	Đ [c]

PD_{5k}	0:26	30	4810	6900 (4210)	8500 (4600)	1.21 (1.09)
PN_{5k}	41:0	104	6130	6080 (4720)	6400 (4900)	1.06 (1.03)
PN_{2k}-*b*-PD_{8k}	21:34	52	12580	9860 (8940)	13000 (10200)	1.32 (1.14)
PN_{5k}-*b*-PD_{5k}	47:27	55	11090	8340 (6860)	9100 (7960)	1.09 (1.16)
PN_{8k}-*b*-PD_{2k}	79:8	72	10220	10720 (9120)	11600 (9200)	1.08 (1.01)
P(N_{5k}-*stat*-D_{5k})	42:25	76	9460	12060 (7490)	15100 (10050)	1.25 (1.34)

[a]DP_N:DP_D and $M_{n,NMR}$ calculated from ^{1}H NMR spectra by comparing integration area of peak **a** corresponding to methyl protons of dodecyl end group at 0.88 ppm and those of signals of **l** and **p** at 3.92 and 3.33 ppm, corresponding to PN (peak **l**) and PD (peak **p**), respectively. [b]T_g measured from DSC measurements, heating rate: 10 °C·min^{-1}, [c]$M_{n,SEC}$, $M_{w,SEC}$ and Đ determined form SEC analyses in DMF with 10 mM LiBr or in THF containing 2 vol.% TEA (the value obtained in THF is given in parenthesis).

3.2. CO_2-switchable thermoresponsiveness of PD homopolymer.

PD homopolymer, a weak polyelectrolyte, is fully soluble in water whatever the pH at low temperature. The apparent p*K*a value of PD_{5k} is 7.25 determined by pH-titration curve (**Figure S11**), and this value is close to the p*K*a values measured for PDEAEMA and PDMAEMA at 7.5 and 7.4 respectively. [22-23] CO_2-responsiveness of PD_{5k} homopolymer was confirmed by recording the pH value during successively bubbling CO_2 and N_2 processes (**Figure 2**). The degree of protonation was calculated by the following equation:

$$Degree\ of\ protonation = \frac{1}{1+10^{pH-pKa}} \qquad \textbf{(eq. 6)}$$

The initial pH value of PD_{5k} solution (1 wt.%) obtained by direct dissolution of polymer in ultra-pure water is 9.3 corresponding to a degree of protonation equal to 0.92%. The addition of CO_2 induces a rapid drop of pH down to 5.5 after 2.5 min with no longer further evolution, while the

degree of protonation rises to around 99%. When N_2 was bubbled for 20 min, the pH of PD_{5k} solution gradually increases to 8.5, while the degree of protonation returns to 5%. Moreover, these variations in pH and/or degree of protonation upon alternately introduction of CO_2/N_2 is repeated for at least two cycles (**Figure S12**), it turns out that CO_2-responsiveness is reversible, making CO_2 superior to the classical pH-sensitive system in which an acid or base solution (e.g. HCl or NaOH) is added to tune the reversibility of the system. Consequently, salt (e.g. NaCl) is produced and accumulated after each cycle.

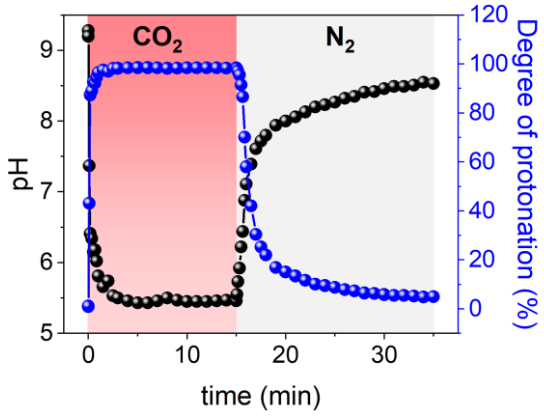

Figure 2. pH value and degree of protonation of PD_{5k} in water upon alternately bubbling CO_2/N_2 ([PD_{5k}] = 0.1 wt.%, gas flow rate: 2 $mL \cdot min^{-1}$).

To further assess the interaction between CO_2 and PD_{5k} homopolymer, we conducted ^1H and ^{13}C NMR spectra in D_2O at 25 °C before and after bubbling CO_2 and N_2. As shown in **Figure 3b**, before exposure to CO_2, PD_{5k} homopolymer presents three prominent signals at 3.32, 2.64 and 1.07 ppm which are attributed to -$C\underline{H}_2CH_2N(CH_2H_3)_2$, -$CH_2C\underline{H}_2N(CH_2CH_3)_2$/-$CH_2CH_2N(C\underline{H}_2CH_3)_2$ and -$C\underline{H}_3$ groups, respectively. Upon 10 min bubbling CO_2, PD_{5k} is protonated, which shifts corresponding signals downfield to 3.56, 3.27 and 1.32 ppm, respectively. Meanwhile, the signal at 160 ppm in ^{13}C NMR spectrum after CO_2 treatment reveals the formation of ammonium bicarbonate (see **Figures 3a** and **3c**).

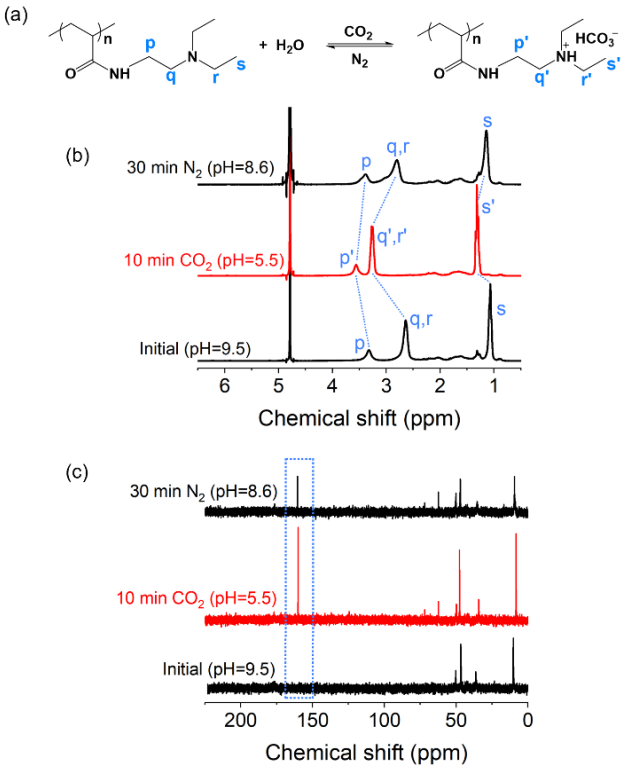

Figure 3. (a) Chemical reaction of PD homopolymer with CO_2 in water. (b) ^{1}H and (c) ^{13}C NMR spectra of PD_{5k} in D_2O recorded at 25 °C upon alternate exposure to CO_2/N_2 ([PD_{5k}] = 1 wt.%, gas flow rate: 10 mL·min^{-1}).

As expected in the case of tertiary amine, no formation of carbamate is evidenced here. [18,19,21] After 30 min bubbling N_2, chemical shifts of these peaks return to 3.39, 2.80 and 1.14 ppm, respectively. This incomplete recovery to the initial position might be ascribed to the existence of residual bicarbonate salt corresponding to a residual protonation degree equal to 5% as mentioned above.

Coexistence of acrylamide and tertiary amine groups within PD_{5k} structure endows the homopolymer with dual thermo- and pH-responsive properties. Thermoresponsiveness and the intensity of response are determined by the degree of protonation of diethylamino groups tuned by system pH. Considering CO_2-induced protonation-deprotonation transition of diethylamino groups and its further effect on solubility of PD chains, turbidimetry measurements were therefore

conducted to study the thermoresponsive properties of PD_{5k} solution before and after bubbling CO_2 or N_2 (**Figure 4a**). Before exposure to CO_2 (pH = 9.3), diethylamino groups in PD_{5k} are not protonated. Thus, PD_{5k} is thermoresponsive and displays a LCST behavior with a measured T_c around 32 °C. After bubbling CO_2, the majority of diethylamino groups become protonated, transmittance remains constant around 100% as PD_{5k} solution was heated from 20 to 80 °C, indicating that PD_{5k} is no longer thermoresponsive. Upon N_2 treatment, LCST behavior of PD_{5k} is recovered with a higher T_c (65 °C) compared to the value in initial solution, this phenomenon is ascribed to the remaining presence of ammonium bicarbonate. [39,44]

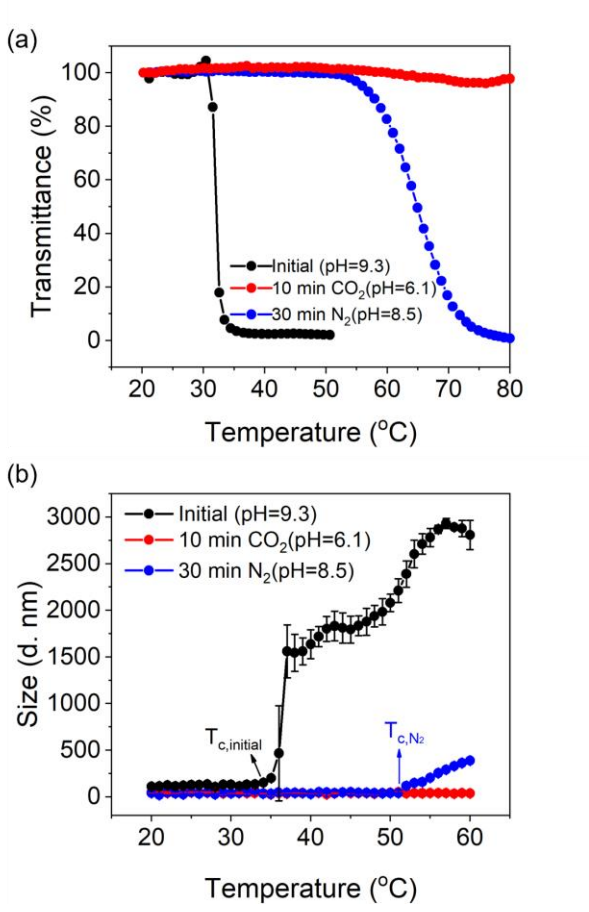

Figure 4. Plots of (a) Transmittance and (b) Number-distributed size versus temperature for PD_{5k} aqueous solution before and after bubbling CO_2 or N_2 ([PD_{5k}] = 1 wt.%, gas flow rate: 10 $mL \cdot min^{-1}$).

CO_2-switchable thermoresponsiveness of PD_{5k} was further investigated by DLS measurements. At 20 °C, PD_{5k} chains in the absence of CO_2 are highly soluble in water, an increase of temperature induces the collapse of PD_{5k} chains. As a result, a drastic change in hydrodynamic size takes place as shown in **Figure 4b**: the hydrodynamic diameter of PD_{5k} solution starts to increase at 34 °C, then undergoes a rapid rise and reaches 1560 nm at 37 °C. The formation of large colloidal structure is not observed after bubbling CO_2 for 10 min. Upon 30 min bubbling N_2, most of charged tertiary amine groups in PD_{5k} return to deprotonated state, thus, thermoresponsive properties of PD_{5k} are recovered with a shift of T_c towards higher temperatures (51 °C) as reported in Zhang's work. [45] The further repeated addition of CO_2/N_2 allows to change the protonation state of tertiary amine functions in a complete reversible way without modification of aggregation properties.[20] In comparison, performing such an addition by the alternative addition of HCl and NaOH led to the formation of NaCl. Its presence results in a progressive shift of measured T_c and a modification of aggregation process measured through turbidimetry measurements (**Figure S13**)

The above investigation on PD homopolymer reveals a strong dependence of thermoresponsive properties upon the protonation degree of polymer chains. In the following we aim at evaluating how the insertion of PD within PN structures affect the thermoresponsiveness of obtained copolymers and how this thermoresponsiveness can be tuned by CO_2 addition/removal. For this, copolymers with a constant molecular weight (10k) but different compositions or architectures (statistical and block) will be compared.

3.3. Reversible CO_2/N_2-response of PN-*b*-PD block copolymers.

Solubility properties. CO_2-responsiveness of PN-*b*-PD was firstly analysed by ^{1}H NMR at room temperature. The interaction sites between CO_2 and PN_{5k}-*b*-PD_{5k} are evidenced in **Figure 5b**. Chemical shifts of -C$\underline{H}_2$CH_2-, -CH_2C$\underline{H}_2$- and -C$\underline{H}_2$CH_3, as well as -C$\underline{H}_3$ in PD_{5k} block upon 10 min bubbling CO_2 move from 3.33, 2.65 and 1.08 ppm to 3.58, 3.28 and 1.33 ppm, then return to 3.43,

2.87 and 1.15 ppm respectively after 30 min N_2 aeration. Moreover, no shifts of signals at 3.89 and 1.15 ppm corresponding to -C<u>H</u>$(CH_3)_2$ and -CH$(C\underline{H}_3)_2$ in PN_{5k} block are observed during the whole process of gas treatment. Similar phenomena were also detected in the cases of PN_{2k}-*b*-PD_{8k} and PN_{8k}-*b*-PD_{2k} (see **Figure S14**).

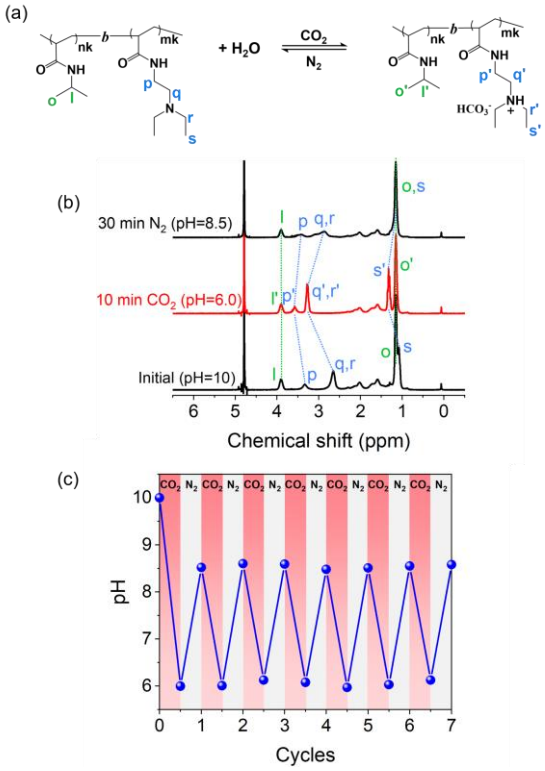

Figure 5. (a) Chemical reaction of PN-*b*-PD with CO_2 in water. (b) ^{1}H NMR spectra of PN_{5k}-*b*-PD_{5k} in D_2O recorded at 25 °C before and after exposure to CO_2 or N_2. (c) pH changes of PN_{5k}-*b*-PD_{5k} system measured at 25 °C upon seven cycles of alternately bubbling CO_2/N_2. ([PN_{5k}-*b*-PD_{5k}] = 1 wt.%, gas flow rate: 10 mL·min^{-1}, bubbling CO_2 and N_2 for 10 and 30 min, respectively)

During bubbling CO_2/N_2 process, the initial pH value around 10, then decreases to 6 upon CO_2 aeration and returns to 8.5 after 30 min N_2 treatment. In the case of PN_{5k}-*b*-PD_{5k} solution, regardless of the initial pH at 10, its pH value switches between 6.0 and 8.5 after cyclically purging CO_2 (for 10 min) and N_2 (for 30 min) respectively (**Figure 5c**). In the case of PN_{2k}-*b*-PD_{8k} and PN_{8k}-*b*-PD_{2k}, a pH window equal to 6.0 - 8.4 and 5.4 - 8.4 respectively upon alternating CO_2/N_2 were measured

(**Figure S15**). These results suggest that CO_2-switchable pH change of PN-*b*-PD solution is fully reversible. [5-7] A similar effect could be obtained by successive addition of acid and base but in this case the repeated cycles would lead to a progressive increase of the ionic strength of the solutions and to an alteration of the thermal properties of the polymers.

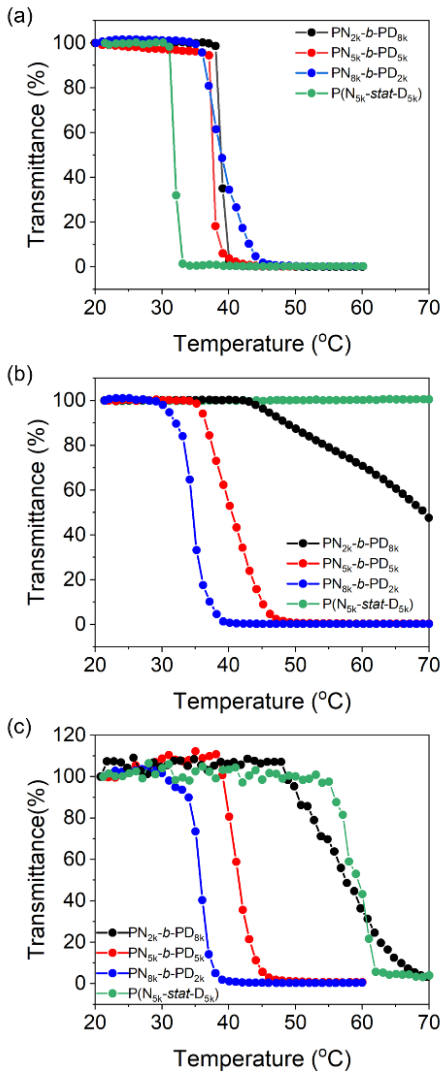

Figure 6. Plots of transmittance *versus* temperature for block and statistical copolymer aqueous solutions (a) before, (b) after bubbling CO_2 and (c) after bubbling N_2 ([P(N-*co*-D)] = 1 wt.%, heating rate: 1 °C·min^{-1}, gas flow rate: 10 mL·min^{-1}, bubbling CO_2 and N_2 for 10 and 30 min, respectively).

CO_2-switchable thermoresponsiveness of P(N-*co*-D) system was further studied by turbidimetry measurements (**Table 2)**. Initially, without CO_2 stimulation, PN and PD blocks are both thermoresponsive with a common T_c equal to 32 °C. From the plot of transmittance vs temperature, only one phase transition temperature was detected whatever copolymer composition or architecture. As shown in **Figure 6a**, the transmittances of all PN-*b*-PD block copolymer solutions start to decrease around 37 °C upon heating and they all undergo a soluble-to-insoluble transition in a relatively narrow temperature range of 38 ± 1 °C, suggests that copolymer composition has a slight effect on T_c for block copolymers. This value, higher than the one measured for PN and PD homopolymers, may be related to a cooperative contribution from both blocks triggering thermal phase transition, which has also been reported in the cases of poly(*N*-isopropylacrylamide)-*block*-poly(*N*-vinylcaprolactam) (PNIPAM-*b*-PVCL) and P(NIPAM-*stat*-VCL). [52-53] Interestingly, T_c value for the statistical copolymer P(N_{5k}-*stat*-D_{5k}) solution is lower than the one measured for the block copolymer PN_{5k}-*b*-PD_{5k} having a with similar composition, i.e. 31 and 37°C respectively. The copolymer architecture has therefore a strong influence on the cloud point values: the statistical insertion of tertiary amine groups disturbs the interaction between the acrylamide moieties and water, resulting in a lowering of measured T_c.

After exposure to CO_2, the pH of polymer solution decreases around 6. Only PN chains remain thermoresponsive, while PD protonated moieties promotes the solubility of whole copolymer in water. As observed in **Figure 6b**, the onset points of transmittance in the cases of PN_{2k}-*b*-PD_{8k}, PN_{5k}-*b*-PD_{5k} and PN_{8k}-*b*-PD_{2k} shift to 43, 35 and 30 °C respectively. The insertion of a charged hydrophilic block induces an increase of measured T_c compared to PN homopolymer. Additionally, in the case of PN_{2k}-*b*-PD_{8k} slightly turbid solutions were obtained upon T_c. This suggests that, during the aggregation process, smaller colloidal structures are formed than for PN_{8k}-*b*-PD_{2k} and PN_{5k}-*b*-PD_{5k}. Moreover, the effect of architecture appears to be of primary importance. Indeed, PN_{5k}-*b*-PD_{5k} remains thermoresponsive, whereas statistical copolymer P(N_{5k}-*stat*-D_{5k}) loses

thermoresponsiveness in the same studied temperature range. After bubbling N_2 (**Figure 6c**), all systems regain their heat-sensitive properties (pH ~ 8.5). However, due to the presence of residual ammonium bicarbonate (protonation degree around 5%), none of the systems can entirely recover to the initial values.

These results indicate that copolymer composition and architecture play a crucial role in CO_2-tunable phase transition temperature. Moreover, the transition temperature of these copolymers can also be tuned by changing the level of protonation of PD moiety.

Table 2. Measurements of T_c (°C) for (co)polymers from turbidimetry measurements.

(Co)polymer	Initial (pH ~ 10)		After bubbling CO_2 (pH ~ 6)		After bubbling N_2 (pH ~ 8.5)	
	$T_{c,onset}$ [a]	$T_{c,ip}$ [b]	$T_{c,onset}$	$T_{c,ip}$	$T_{c,onset}$	$T_{c,ip}$
PD_{5k}	30[d]	32[d]	/[c]	/[c]	54	65
PN_{2k}-*b*-PD_{8k}	38	39	43	/[c]	48	/[c]
PN_{5k}-*b*-PD_{5k}	37	38	35	40	38	41
PN_{8k}-*b*-PD_{2k}	35	37	30	34	30	36
P(N_{5k}-*stat*-D_{5k})	31	32	/[c]	/[c]	56	60

[a]$T_{c,onset}$ determined from temperature where transmittance of copolymer solution starts to decrease. [b]$T_{c,ip}$ determined from the inflection point of transmittance curve. [c]Not observed in the studied temperature range of 20 - 70 °C. [d]Initial pH value of PD_{5k} solution was 9.3. Turbidimetry measurements were performed with a heating rate of 1 °C·min^{-1}. Gas flow rate was 10 mL·min^{-1}, 10 and 30 min for bubbling CO_2 and N_2 respectively.

Aggregation properties. The modifications of the behaviour in solution of these polymers induced by changes in temperature are then studied for the different compositions of the synthesized polymers. TEM, DLS and SAXS measurements were carried out to investigate the structure and the size of aggregates.

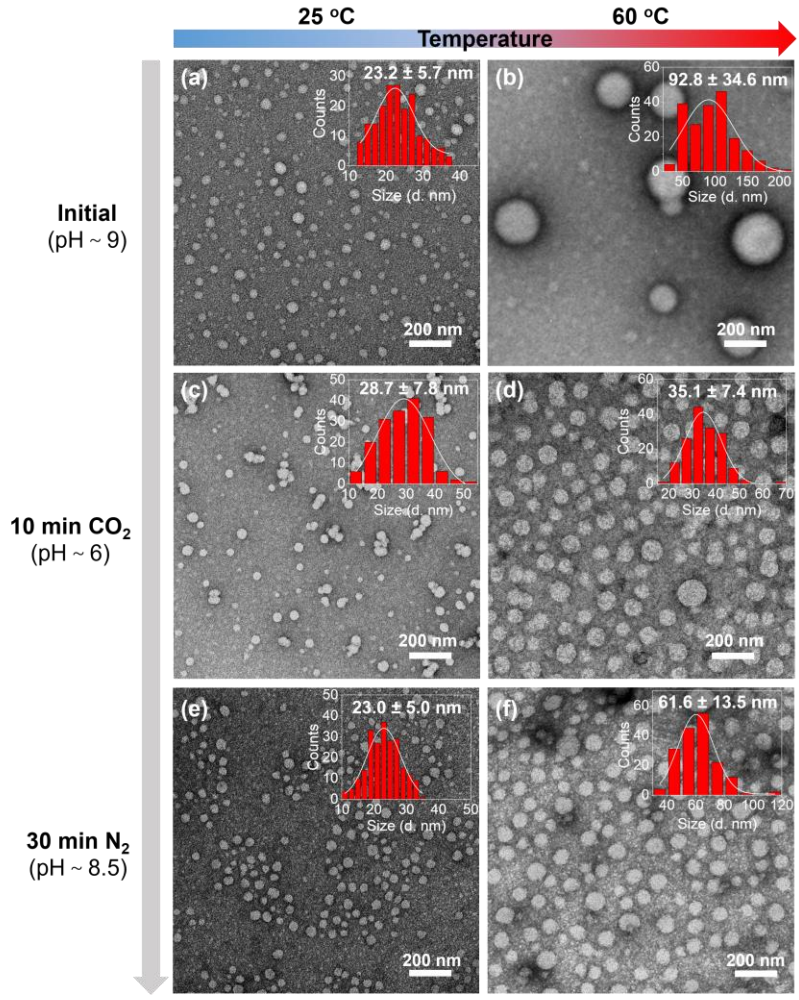

Figure 7. TEM images of PN_{5k}-*b*-PD_{5k} aggregates formed before, after bubbling CO_2 and after bubbling N_2 at 25 and 60 °C ([PN_{5k}-*b*-PD_{5k}] = 0.1 wt.%, gas flow rate: 10 mL·min^{-1}, 10 and 30 min for bubbling CO_2 and N_2 respectively. All samples were stained with 2 wt.% uranyl acetate before TEM observation).

At low pH the polymer P(N_{5k}-stat-D_{5k}) remains fully soluble and no aggregates can be evidenced. At pH 9.6, light scattering measurement evidences the formation of the large aggregates that quickly precipitates (**Figure S16**). Therefore, the studies on self-assemblies' properties were only conducted on block copolymers.

At pH ~ 10 and 25°C ($T < T_c$), PN_{5k}-*b*-PD_{5k} forms spherical structure with an average diameter of 23.2 ± 5.7 nm as evidenced by TEM images (**Figure 7a**). SAXS curves indicate the presence of nano-objects with a radius of gyration (R_g) equal to 3.5 ± 1 nm (**Figure 8a**). Interestingly the Guinier region is followed by a power-law trend $I(q) \sim q^{-\alpha}$, with $\alpha = 1.6$ indicating swollen chains in good solvent.[50] These radii of gyration have already been reported for assemblies of amphiphilic PNIPAM described as hairy micelles.[53] A model for star-like polymers fits well our data: by fixing R_g value, the number of arms is found equal to 1.5, indicating the coexistence of star-like nano-objects and free polymer chains. The hydrodynamic radius i.e. 24 ± 5 nm (**Figure S17**) is in accordance with what found in the literature.[55] When temperature is increased to 60 °C (pH 10), SAXS profile completely changes and large structures are formed in solution (**Figure 8a**). Indeed, no Guinier region is observed, the signature of the polymeric nature is lost at high-q as the polymer is dehydrated and densely packed and only an extended Porod region with a slope of -4 is present : at a temperature above T_c, both PN and PD chains collapse and become insoluble in water. Spherical aggregates with an average diameter equal to 92.8 ± 34.6 nm and a hydrodynamic diameter equal to 170 ± 40 nm are thus detected by TEM and DLS measurements respectively (**Figure 7b** and **Figure S17**).

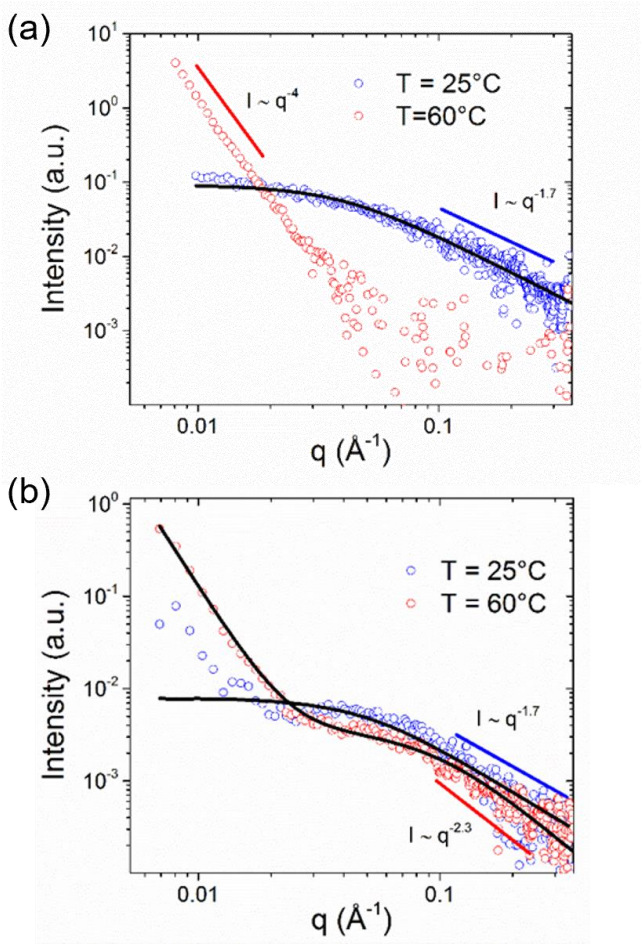

Figure 8. Small-angle X-ray scattering (SAXS) patterns recorded for 1 wt.% aqueous dispersion of PN_{5k}-*b*-PD_{5k} at 25 and 60 °C (a) before (pH ~ 10) and (b) after bubbling CO_2 (pH ~ 6). CO_2 flow rate: 10 mL·min^{-1}, bubbling time: 10 min).

After exposure to CO_2 during 10 min, the pH of solution drops down to 6.0 and only PN group remains thermoresponsive while PD is in its protonated form. At 25 °C, spherical aggregates are still evidenced by TEM images (**Figure 7c**) with slightly larger diameter i.e. 28.7 ± 7.8 nm than the one measured without CO_2 treatment (D_h = 23 ± 5 nm). Electrostatic repulsion among the positive charged PD chains might induce the expansion of aggregates. SAXS curves show the main features already observed at pH 10, a R_g of few nanometres (2.7 ± 0.8 nm) is slightly higher than what expected for free polymer chains in solution, and a high q trend of chains swollen by the solvent (**Figure 8b**). A fit using a form factor of star-polymers indicates a low aggregation number (1.5)

and coexistence of small star-like micelles and free polymer chains. On heating to 60 °C, the sample gets turbid due to the presence of large spherical aggregates with a diameter equal to 35.1 ± 7.4 nm determined from TEM measurements (**Figure 7d**), which is significantly smaller than the ones measured prior to the exposure to CO_2. Indeed, PN chains collapse upon increasing temperature, whereas protonated PD chains remain hydrated and help to stabilize smaller colloidal structures in solution. These assemblies exhibit larger size than what measured by SAXS technology. We use a model for clusters of polymer chains developed by Hammouda [50] and find a correlation length for the polymer of 1 ± 0.3 nm and a power-law exponent 2.3 ± 0.1 indicating polymers are in semi-dilute solutions. Interestingly, the polymeric features of the assemblies formed above LCST are not completely lost for this sample, which is not the case for the sample without CO_2 stimulation.

Upon 30 min bubbling N_2, the system pH returns to 8.5, thermoresponsiveness of PD block is recovered. At 25 °C, the diameter of spheres is almost recovered to the initial size through TEM or DLS observations (23.0 ± 5.0 nm, **Figure 7e**). At 60 °C, PD shrinks along with the collapse of PN block and spheres with an average diameter of 61.6 ± 13.5 nm in dried state are detected (**Figure 7f**).

The aggregates obtained show no significant morphological change for a chosen pH and temperature condition after a cooling/heating cycle or after CO_2/N_2 bubbling cycle (**Figure S18 and S19**).

Similar trends have been observed concerning the behavior of PN_{2k}-*b*-PD_{8k} and PN_{8k}-*b*-PD_{2k} in solution (**Figures S20** and **S21**). The diameter of the aggregates in presence of CO_2 at 60 °C seems to decrease significantly with an increase of PD content (**Figure 9**), this could be related to the ability of the protonated chains of PD to stabilize colloids by electrostatic effect: an increase of their proportion favors the stabilization of colloids with smaller size. The evolution of the hydrodynamic diameters shows the same tendency as those observed in the electron microscopy images (Figure 9). As expected the values of the hydrodynamic diameters are significantly higher than the

measurements obtained in a dried state in TEM. Moreover, these high values suggest the presence of polydisperse aggregates in solution.

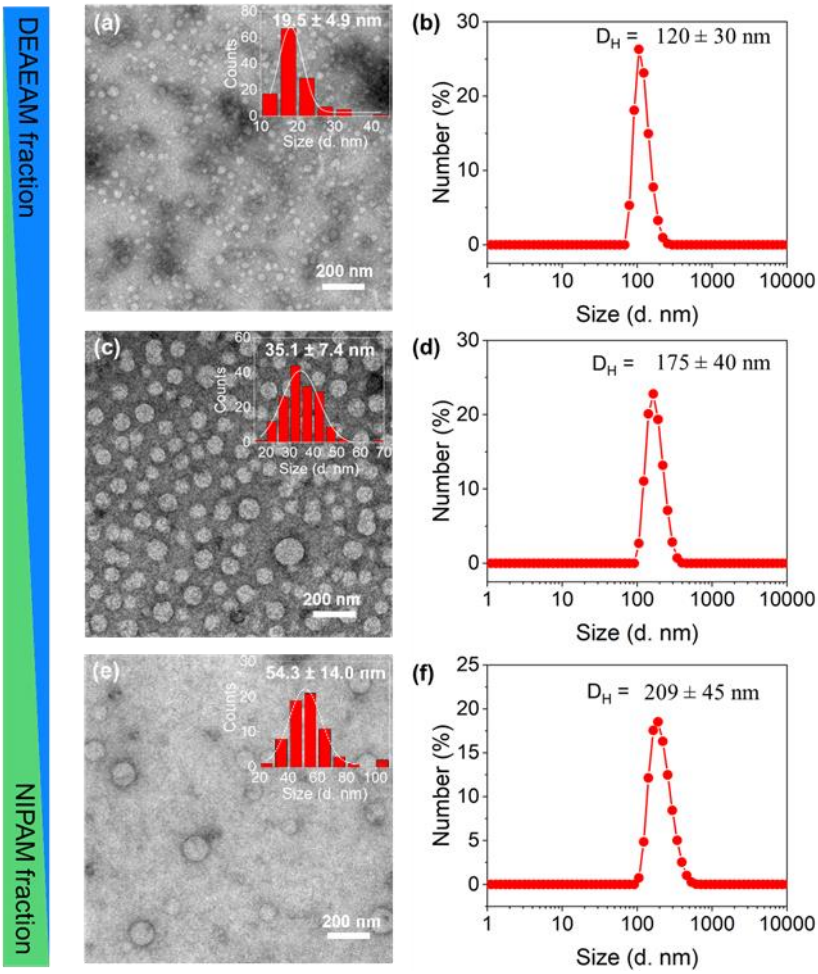

Figure 9. TEM images and number-distributed hydrodynamic size of (a, b) PN_{2k}-*b*-PD_{8k}, (c, d) PN_{5k}-*b*-PD_{5k} and (e, f) PN_{8k}-*b*-PD_{2k} aggregates formed at 60 °C after exposure to CO_2 ([PN-*b*-PD] = 0.1 wt.%, CO_2 flow rate: 10 mL·min^{-1}, bubbling time: 10 min).

Based on the above results, a mechanism of the formation of different colloids observed at different studied temperatures with/without CO_2 stimulation can be proposed as follows (**Scheme 4**). In initial solution (pH ~ 9), both PN and PD blocks are thermoresponsive. At 25 °C ($T < T_c$), block copolymer PN-*b*-PD forms spherical micelles with a core of hydrophobic -$C_{12}H_{25}$ group and

a corona of PN and PD blocks. This structure is similar to the ones previously observed in the case of PNIPAM-based surfactant with a similar hydrophobic alkyl chain as the terminal group.[55]

At 60 °C, both PN and PD blocks dehydrate and collapse, the formed dense and hydrophobic structures are prone to aggregate in aqueous solution (**Scheme 4 left**). However, the remaining carboxylate terminal function might explain the relative colloidal stability of such structures. Upon CO_2 treatment (pH ~ 6), PD block is protonated, the electrostatic repulsion among charged PD chains causes an expansion of corona region, and induces a slight swelling of spherical nanoparticles (**Scheme 4 bottom**). When temperature increases above T_c, PN chains shrink whereas charged PD block remains hydrated. Therefore, the copolymer forms aggregates, in which $-C_{12}H_{25}$ group and dehydrated PN forms the core, while charged PD block forms the corona. In agreement with the proposed mechanism, an increase in zeta potential from +20 to +50 mv is measured when the temperature increase from 20 to 60°C. The observed size is compatible with the possible association of several small aggregates (**Scheme 4 right**).

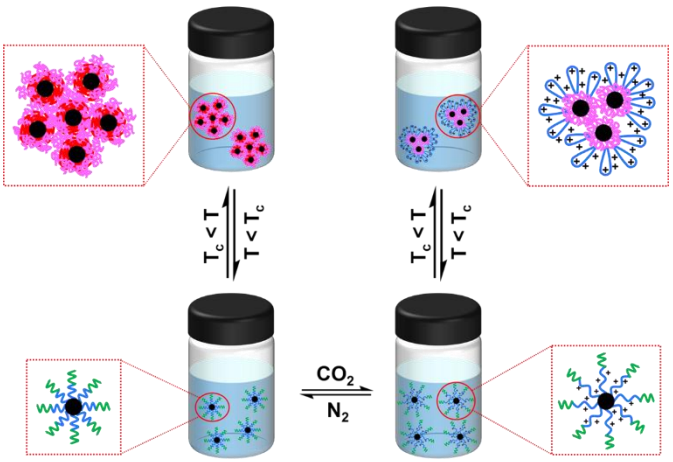

Scheme 4. Schematic illustration of self-organization of PN-*b*-PD in water triggered by temperature and CO_2.

4. Conclusions

In this article, the insertion of DEAEAM into PNIPAM structure by Reversible Addition-Fragmentation chain Transfer (RAFT) polymerization was studied and makes it possible to obtain a series of copolymers with various compositions and architectures. CO_2 addition/removal induces a reversible protonation/deprotonation transition of DEAEAM units, which results in tunable thermoresponsive properties of the synthesized polymers. For a given composition, the architecture of the copolymer (statistical, block) critically affects the cloud point temperature and the structure of colloids obtained in solution. The statistical copolymer is no longer thermoresponsive upon CO_2 exposure, whereas block one with a similar composition keeps its responsiveness, which depends on the protonation degree. Additionally, these results illustrate how it is possible through chemical engineering and the use of CO_2 as an innovative and ecological trigger to easily and reversibly modulate the properties (solubility, self-assembly behavior) of these smart materials in aqueous media. [4,5,56]

Author Contributions

N. Lauth-de Viguerie and J.-D. Marty conceived the idea and supervised this project. F. Yin performed the experiments and wrote the first draft of the paper. B. Lonetti contributed to the SAXS measurement and analyses. All authors participated in evaluating the results and commented on the manuscript.

Conflicts of interest

There are no conflicts to declare.

Acknowledgements

The authors acknowledge CNRS and China Scholarship Council (CSC) for the financial support. The authors thank P. Roblin for the access to SAXS facilities and B. Payré and D. Goudenèche for TEM access at CMEAB.

References

[1] A. Darabi, P.G. Jessop, M.F. Cunningham, Chem. Soc. Rev. 45 (2016) 4391-436.

[2] B. Jiang, Y. Zhang, X. Huang, T. Kang, S.J. Severtson, W.-J. Wang, P. Liu, Ind. Eng. Chem. Res. 58 (2019) 15088-15108.

[3] Q. Yan, Y. Zhao, Chem. Commun. 50 (2014) 11631-11641.

[4] M.F. Cunningham, P.G. Jessop, Macromol. React. Eng. 16 (2022) 2200031.

[5] M.F. Cunningham, P.G. Jessop, Macromolecules 52 (2019) 6801-6816.

[6] Y. Hoshino, K. Imamura, M Yue, G. Inoue,Y. Miura, J. Am. Chem. Soc. 134 (2012) 18177-18180

[7] H. Liu, S. Lin, Y. Feng, P. Theato, Polym. Chem. 8 (2017) 12-23.

[8] B. Razavi, A. Abdollahi, H. Roghani-Mamaqani, M. Salami-Kalajahi, Mater. Sci. Eng. C 109 (2020) 110524.

[9] S. Lin, X. Huang, R. Guo, S. Chen, J. Lan, P. Theato, J. Polym. Sci. A Polym. Chem. 57 (2019) 1580-1586.

[10] J. Han, Z. Du, W. Zou, H. Li, C. Zhang, Ind. Eng. Chem. Res. 54 (2015) 7623-7631.

[11] M. Yue, Y. Hoshino, Y. Miura, Angew. Chem. Int. Ed. 53 (2014), 2654-2657

[12] Y. Wang, S. Yang, J. Zhang, Z. Chen, B. Zhu, J. Li, S. Liang, Y. Bai, J. Xu, D. Rao, L. Dong, C. Zhang, X. Yang, Nat. Commun. 14 (2023) 1108.

[13] H. Che, M. Huo, L. Peng, T. Fang, N. Liu, L. Feng, Y. Wei, J. Yuan, Angew. Chem. Int. Ed. 54 (2015) 8934-8938.

[14] Q. Yan, J. Wang, Y. Yin, J. Yuan, Angew. Chem. Int. Ed. 52 (2013) 5070-5073.

[15] Q. Yan, Y. Zhao, Angew. Chem. Int. Ed. 52 (2013) 9948-9951.

[16] F.S. Pereira, E.R. deAzevedo, E.F. da Silva, T.J. Bonagamba, D.L. da Silva Agostíni, A. Magalhães, A.E. Job, E.R. Pérez González, Tetrahedron 64 (2008) 10097-10106.

[17] S. Lin, J. Shang, P. Theato, ACS Macro Lett. 7 (2018) 431-436.

[18] D. Han, X. Tong, O. Boissière, Y. Zhao, ACS Macro Lett. 1 (2012) 57-61.

[19] D. Nagai, A. Suzuki, Y. Maki, H. Takeno, Chem. Commun. 47 (2011) 8856-8858.

[20] Q. Yan, Y. Zhao, J. Am. Chem. Soc. 135 (2013) 16300-16303.

[21] M.F. Cunningham, P.G. Jessop, Eur. Polym. J. 76 (2016) 208-215.

[22] P. van de Wetering, E.E. Moret, N.M.E. Schuurmans-Nieuwenbroek, Bioconjugate Chem. 10 (1999) 589−597.

[23] V. Bütün, S.P. Armes, N.C. Billingham, Polym. 42 (2001) 5993-6008.

[24] T. Thavanesan, C. Herbert, F.A. Plamper, Langmuir 30 (2014) 5609-5619.

[25] D. Han, O. Boissiere, S. Kumar, X. Tong, L. Tremblay, Y. Zhao, Macromolecules 45 (2012) 7440-7445.

[26] H. Liu, Z. Guo, S. He, H. Yin, C. Fei, Y. Feng, Polym. Chem. 5 (2014) 4756-4763.

[27] D. Zhang, Y. Fan, H. Chen, S. Trépout, M.-H. Li, Angew. Chem. Int. Ed. 58 (2019) 10260-10265.

[28] F. Yin, H.H. Nguyen, O. Coutelier, M. Destarac, N. Lauth-de Viguerie, J.-D. Marty, Colloids Surf. A Physicochem. Eng. Asp. 630 (2021) 127611.

[29] X. Zhao, O. Coutelier, H.H. Nguyen, C. Delmas, M. Destarac, J.-D. Marty, Polym. Chem. 6 (2015) 5233-5243.

[30] W. Steinhauer, R. Hoogenboom, H. Keul, M. Moeller, Macromolecules 46 (2013) 1447-1460.

[31] A. Halperin, M. Kröger, F.M. Winnik, Angew. Chem. Int. Ed. 54 (2015) 15342-15367.

[32] F. Yin, J.S. Behra, M. Beija, A. Brûlet, J. Fitremann, B. Payré, S. Gineste, M. Destarac, N. Lauth-de Viguerie, J.-D. Marty, J. Colloid Interface Sci. 578 (2020) 685-697.

[33] M. Heskins, J.E. Guillet, J. Macromol. Sci. A 2 (1968) 1441-1455.

[34] S. Sistach, M. Beija, V. Rahal, A. Brûlet, J.-D. Marty, M. Destarac, C. Mingotaud, Chem. Mater. 22 (2010) 3712-3724.

[35] Z.-P. Xiao, Z.-H. Cai, H. Liang, J. Lu, J. Mater. Chem. 20 (2010) 8375.

[36] A. Feng, C. Zhan, Q. Yan, B. Liu, J. Yuan, Chem. Commun. 50 (2014) 8958-8961.

[37] B.-w. Liu, H. Zhou, S.-t. Zhou, H.-j. Zhang, A.-C. Feng, C.-m. Jian, J. Hu, W.-p. Gao, J.-y. Yuan, Macromolecules 47 (2014) 2938-2946.

[38] W. Yuan, J. Shen, H. Zou, RSC Adv. 5 (2015) 13145-13152.

[39] K. Wang, Z. Song, C. Liu, W. Zhang, Polym. Chem. 7 (2016) 3423-3433.

[40] C. Luo, W. Fu, Z. Li, B. Zhao, Polymer 101 (2016) 319-327.

[41] X. Jiang, C. Feng, G. Lu, X. Huang, ACS Macro Lett. 3 (2014) 1121-1125.

[42] X. Jiang, C. Feng, G. Lu, X. Huang, Polymer 64 (2015) 268-276.

[43] Z. Shahrbabaki, F. Oveissi, S. Farajikhah, M.B. Ghasemian, R.D. Jansen-van Vuuren, P.G. Jessop, J. Yun, F. Deghani, S. Naficy, ACS Omega 7 (2022) 22232-22243.

[44] P. Schattling, I. Pollmann, P. Theato, React. Funct. Polym. 75 (2014) 16-21.

[45] Z. Song, K. Wang, C. Gao, S. Wang, W. Zhang, Macromolecules 49 (2016) 162-171.

[46] F. Yin, P. Laborie, B. Lonetti, S. Gineste, Y. Coppel, N. Lauth-de Viguerie, J.-D. Marty, Macromolecules 56 (2023), 3703-3720

[47] X. Guan, L. Meng, Q. Jin, B. Lu, Y. Chen, Z. Li, L. Wang, S. Lai, Z. Lei, Macromol. Mater. Eng. 303 (2018) 1700553.

[48] J. Lee, K.H. Ku, C.H. Park, Y.J. Lee, H. Yun, B.J. Kim, ACS Nano 13 (2019) 4230-4237.

[49] D. Richter, B. Farago, J.S. Huang, L.J. Fetters, B. Ewen, Macromolecules 22 (1989) 468-472.

[50] B. Hammouda, D.L. Ho, S. Kline, Macromolecules 37 (2004) 6932-6937.

[51] A.P. Narrainen, S. Pascual, D.M. Haddleton, J. Polym. Sci. A Polym. Chem. 40 (2002) 439-450.

[52] L. Hou, P. Wu, Soft Matter 10 (2014) 3578-3586.

[53] L. Hou, P. Wu, Soft Matter 11 (2015) 2771-2781.

[54] P.A. FitzGerald, S. Gupta, K. Wood, S. Perrier, G.G. Warr, Langmuir 30 (2014) 7986-7992.

[55] J.P. Patterson, E.G. Kelley, R.P. Murphy, A.O. Moughton, M.P. Robin, A. Lu, O. Colombani, C. Chassenieux, D. Cheung, M.O. Sullivan, T.H. Epps, R.K. O'Reilly, Macromolecules 46 (2013) 6319-6325.

[56] B. Pang, Y. Yu, W. Zhang, Macromol. Rapid Commun. 42 (2021) 2100504.